International Journal of Computational and Experimental Science and ENgineering
(IJCESEN)

Vol. 12-No.2 (2026) pp. 597-606
http://www.ijcesen.com

ISSN: 2149-9144

Research Article

Energy Management Optimization of Hybrid Sustainable Microgrids Enriched with Renewable Energy Sources Using Nature-inspired Intelligence Algorithm

Ilhem Ahmed Hazila[1]*, Bilel Ayachi[2], Nabil Mezhoud[3], Farouk Boukhenoufa[4], Ahmed Bahri[5]

[1]Electrical Engineering Department, Faculty of Technology, LES Laboratory, Université 20 Août 1955-Skikda, Algeria
* **Corresponding Author Email:** i.ahmedhazila@univ-skikda.dz - **ORCID:** 0009-0001-1071-8951

[2]Electrical Engineering Department, Faculty of Technology, LES Laboratory, Université 20 Août 1955-Skikda, Algeria
Email: b.ayachi@univ-skikda.dz - **ORCID:** 0000-0002-7170-0085

[3]Electrical Engineering Department, Faculty of Technology, LES Laboratory, Université 20 Août 1955-Skikda, Algeria
Email: n.mezhoud@univ-skikda.dz - **ORCID:** 0000-0002-9383-2097

[4]Electrical Engineering Department, Faculty of Technology, LES Laboratory, Université 20 Août 1955-Skikda, Algeria
Email: f.boukhenoufa@univ-skikda.dz - **ORCID:** 0000-0003-1018-8249

[5]Faculté des Sciences et de la Technologie, MESTE Laboratory, Université de Ghardaia, Algeria
Email: bahri.ahmed@univ-ghardaia.edu.dz - **ORCID:** 0009-0000-0016-4994

Article Info:

DOI: 10.22399/ijcesen.5252
Received : 15 March 2026
Revised : 15 May 2026
Accepted : 20 May 2026

Keywords

Energy Management optimization
Renewable Energy Sources
Microgrid
Energy Storage Systems
Gorilla Troops Optimizer

Abstract:

Given the need to realize the full operational benefits of microgrids, such as improved profitability, enhanced reliability, enhanced energy efficiency and quality, reduced dependence on the main grid, reduced losses and costs, and clean environments, the deployment of distributed generators, has increased significantly, particularly those powered by renewable energy sources such as wind and solar. Widespread reliance on renewable energy in microgrids avoids rising fuel prices and provides a sustainable alternative to future fossil fuel depletion. This study employs the Gorilla Troops Optimizer (GTO), a widely recognized bio-inspired intelligent optimization technique, to address the Optimal Energy Management (OEM) challenge in a microgrid (MG) powered by renewable energy sources (RES). The proposed GTO-based strategy was evaluated using a benchmark microgrid integrating multiple renewable and distributed energy technologies, including wind turbines (WT), photovoltaic (PV), fuel cells (FC), microturbines (MT), diesel electric generators (DEG), and energy storage systems (ESS). The obtained findings demonstrate strong performance, reliability, and efficiency of the proposed method in effectively handling the OEM problem.

1. Introduction

Electricity demand continues to grow due to urban expansion, digital technologies, and industrial progress [1]. Consequently, renewable energy especially solar PV and wind power has gained major attention, leading to higher RES integration into power networks.
In recent years, distributed generation (DG) has expanded considerably. Renewable DG units such as PV and WT depend on weather and site conditions, whereas conventional sources such as FC, MT, and DEG ensure dependable generation and flexible grid connection [2, 3].
Proper management of DG enhances system reliability, efficiency, and power quality while minimizing energy losses and environmental impact. A MG enables the coordinated control of energy storage and flexible loads, operating either autonomously or connected to the utility grid [4, 5].
In recent years, population-based and evolutionary optimization techniques have been successfully adopted to enhance EMO performance [6]-[9]. Human-related swarm intelligence algorithms like Shuffled frog leaping [10], teaching learning-based optimization [11], biogeography-based optimization [12], league championship algorithm [13], harmony search [14], imperialistic competition [15], and sine-cosine algorithm [16] are applied for various EMO.
Swarm-based optimization techniques, including particle swarm optimization [17], artificial bee colony [18], ant colony optimization [19],

glowworm swarm optimization [20], artificial hummingbird algorithm [21], and crayfish optimization algorithm [22], have been applied to reduce and optimize energy management in MGs.
Physics-inspired optimization methods, including gravitational search algorithms [23], black hole optimization [24], wind-driven optimization [25], gradient-based optimizer [26], and flow direction algorithm [27], also address the EMO in MGs.
A very large number of bio and nature-inspired approaches used to address EMO. Among them are the firefly algorithm [28], gray goose optimization [29], gray wolf optimization [30], whale optimization algorithm [31], bacteria search [32], cuckoo search [33], squid algorithm [34], moth swarm algorithm [35], African eagle optimization [36], gorilla swarm optimization [37], marine predator algorithm [38], ant lion optimization [39], and dragonfly algorithm [40].

2. Problem formulation

2.1 Objective function

In general, the EMO can be formulated as[17].

$$\min_u F = \min_u \sum_{t=1}^{nt} \sum_{i=1}^{ng} \left[B_{gi}\left(P_{gi}^t\right) + EMP^t P_{Utility}^t \right] \quad (1)$$

$f(x,u)$ is the MG total operation cost. $P_{Utility}^t$ is the utility power. nt and ng are, respectively, total time total number of DGs. P_{gi}^t, B_{gi} and $EMP^t$are the generating reel power, the DG bid and the energy market price [41], [42].

2.2 Constraints

2.2.1 Power balance constraints (PBC)

The constraints power balance is as follows

$$\sum_{i=1}^{ng} P_{gi}^t + P_{Utility}^t = \sum_{l=1}^{nl} P_{L_l}^t \quad (2)$$

$P_{L_l}^t$ is the tenth loads level, while *nl* is the total number of loads levels.

2.2.2 Capacity of generation power

The generation active powers of every MG, including the utility grid are

$$P_{gi\_min}^t \le P_{gi}^t \le P_{gi\_max}^t \quad (3)$$

$$P_{Utility\_min}^t \le P_{Utility}^t \le P_{Utility\_max}^t \quad (4)$$

$P_{Utility\_min}^t$, $P_{Utility\_max}^t$, $P_{gi\_min}^t$, and $P_{gi\_max}^t$ are, respectively, the powers limits of DG and utility.

2.2.3 Constraints of reserve spinning

To ensure compliance with the reserve requirement, the inequality condition below must be fulfilled [43].

$$\sum_{i=1}^{ng} P_{gi\_max}^t + P_{Utility\_max}^t = \sum_{l=1}^{nl} P_{L_l}^t + RS^t \quad (5)$$

RS^t is the spinning reserve programmed at time *t*.

2.2.4 Dynamic operation and limits of storage

For a standard battery, the power limits during each interval time t are as follows [44].

$$P_{ESS\_min}^t \le P_{ESS}^t \le P_{ESS\_max}^t \quad (6)$$

Here, $P_{ESS\_min}^t$ and $P_{ESS\_max}^t$ are the minimum and maximum allowable charging/discharging power levels of ESS [45]

$$SOC_{ESS}^{t+1} = SOC_{ESS}^t - \frac{\eta_{ESS}^t P_{ESS}^t}{C_{ESS}} \quad (7)$$

$$SOC_{ESS\_min}^t \le P_{ESS}^{t+1} \le P_{ESS\_max}^t \quad (8)$$

SOC_{ESS}^t is the state of charge of ESS, η_{ESS}^t is the efficiency of ESS, C_{ESS} is the capacity of ESS and $SOC_{ESS\_min}^t$ and $SOC_{ESS\_max}^t$ are the SOC minimum and maximum limits of ESS at time t [44]. Equation (7) describes the charging and discharging behavior of the ESS state of charge (SOC), where the SOC rises during charging and declines during discharging. Accordingly, the EMS optimization process determines the variables P_{gi}^t, P_i^t, P_{ESS}^t and SOC_{ESS}^t over the scheduling horizon

2.2.5 Active power from (to) utility

The utility power is calculated as

$$P_{Utility}^t = \sum_{l=1}^{nl} P_{L_l}^t - \sum_{i=1}^{ng} P_{gi}^t \quad (9)$$

We verify that the result P_{gi}^t satisfies constraint (9). Consequently, $P_{Utility\_lim}^t$ is defined as

$$P_{Utility\_lim}^t = \begin{cases} P_{Utility\_max}^t & if \quad P_{Utility}^t > P_{Utility\_max}^t \\ P_{Utility\_lim}^t & if\ P_{Utility\_lim}^t > P_{Utility\_min}^t \\ P_{Utility}^t\ if\ P_{Utility\_min}^t \le P_{Utility\_lim}^t \le P_{Utility\_max}^t \end{cases} \quad (10)$$

2.3 Bids calculation of distributed generation

The DG bids are viewed as

$$B_{gi} = a_i P_{gi}^2 + b_i P_{gi} + c_i \quad (11)$$

2.3.1 Fuel cell and micro-turbine

The bids of FC and MT in ($/h) are computed as

$$B_g = C_{fuel}\left(\frac{P_g}{\eta_g}\right) + C_{inv} \quad (12)$$

P_g and η_g represent the DG generation power and efficiency. C_{fuel} and C_{inv} are the fuel price in ($/kWh) and investment cost in ($/h). C_{inv} is calculated in function of annual AP in (kWh/kW), DG nominal power in (kW), and the annual cost (AC) in ($/kW-year) as follows [5], [46]-[48]

$$C_{inv} = AC(P_{g_{nom}}/AP) \quad (13)$$

$$AC = (i(1+i)^n/(1+i)^n - 1)IC \quad (14)$$

i denotes the interest rate, n represents the project lifetime in years, and IC refers to the DG installation cost. These parameters are estimated by approximating the MT electrical efficiency characteristics using manufacturer-provided data.

2.3.2 Photovoltaic and wind turbines

The bidding models of PV and WT systems are formulated using the annualized cost (AC) and annual production (AP), as expressed in Eqs. (13) and (14). The PV output, P_{PV} is computed as

$$P_{PV} = P_{STC}\frac{I_S}{1000}[1 + \gamma(T_C - 25)] \quad (15)$$

P_{STC} denotes the maximum output power under standard test conditions (STC), γ is the coefficient temperature of PV module, and T_c is the PV cell temperature in $(°C)$. T_c is computed based on the Nominal Operating Cell Temperature (T_{NOCT})

$$T_c = T_a + \frac{I_S}{800}(T_{NOCT} - 20) \quad (16)$$

T_a is the ambient temperature in (°C).
The WT output power characteristic can be represented as follows

$$P_{WT}^t \begin{cases} 0 \\ \frac{v^2 - v_{ci}^2}{v_{nom}^2 - v_{ci}^2} P_{WT_{nom}} \\ P_{nom} \end{cases} \begin{cases} if \ v \le \ v_{ci} \ and \ v \ge v_{co} \\ if \ v_{ci} < v < v_{nom} \\ if \ v_{nom} < v \le v_{co} \end{cases} \quad (17)$$

$P_{WT_{nom}}$, v_{nom} , v_{ci} and v_{co} are, respectively, denote the rated power, rated wind speed, cut-in speed, and cut-out speed of the wind turbine, respectively, while P_{WT} represents the generated wind power [50]-[51].

2.3.3 Diesel Generators (DEG)

The fuel consumption characteristic of DEG is [40]

$$Fuel_{DEG} = a_{fuel}P_{DEG}^2 + b_{fuel}P_{DEG} + c_{fuel} \quad (18)$$

$Fuel_{DEG}$ is the consumed fuel (L/h); P_{DEG} is the DEG generating power; a_{fuel}, b_{fuel} and c_{fuel} are consumption fuel coefficients. The DEG bids is

$$B_{DEG} = C_{fuel}Fuel_{DEG} + C_{inv} \quad (19)$$

C_{inv} is the investment cost C_{fuel} is the diesel price

2.3.4. Utility grid

Market energy costs in ($/h) of utility can be represented as

$$P_{g\_Utility} = a + bP_{g\_Utility} + cP_{g\_Utility}^2 \quad (20)$$

$P_{g\_Utility}$ is the utility power and a, b and c are the cost coefficients.

3. Gorilla Troops Optimizer

In June 2021, Abdollahzadeh et al. [52] introduced a groundbreaking optimization technique called the Gorilla Troops Optimizer (GTO). This algorithm draws inspiration from the intricate social dynamics observed within gorilla communities in the wild. The behavioral framework of GTO is rooted in five core strategies that mirror how gorillas interact and organize in their natural habitat. These behaviors are: exploring unfamiliar areas, approaching other gorilla groups, navigating toward a known target, following the dominant silverback, and engaging in rivalry for adult-females.
These behavioral analogs form the foundation of the algorithm's dual-phase optimization approach, which includes both exploration and exploitation [37]. The initial thé strategies seeking unknown regions, moving toward other troops, and heading toward a specific location drive the exploration component. Conversely, the last two behaviors aligning with the silverback and competing for mates serve to guide the exploitation phase of the search process [53], [54].
One striking trait of gorillas is their exceptional cognitive ability. Recent studies even suggest gorillas might possess higher problem-solving intelligence than humans in certain contexts. They are capable of using rudimentary tools and acquiring sign language skills. This intellectual capacity enables them to explore diverse regions effectively without being easily trapped in suboptimal solutions a critical attribute mirrored in mechanics of search.
Within a gorilla group, each member plays a distinct role, with the silverback taking the lead. This central figure is responsible for the cohesion, protection, and direction of the group, managing conflicts and guiding the troop toward food sources and safer locations. These roles are reflected in GTO's structure, where each gorilla symbolizes a potential solution, and the most promising solution assumes the role of the silverback.
To grasp the GTO's working mechanism more clearly, the following sections elaborate on how these exploration and exploitation strategies interact to optimize complex problems.

3.1 Phase of Discovery: Exploration phase

Within the GTO framework, every gorilla symbolizes a potential answer to the optimization challenge, and at any given point in the process, the Silverback gorilla stands out as the top-performing solution. This discovery phase hinges on three core instinctive behaviors: one, an exploratory leap into uncharted territory to amplify the algorithm's ability to navigate unknown solution regions; two, coordinated movement with other gorillas to strike a dynamic equilibrium between exploring new areas and refining existing ones; and three, purposeful migration toward a known target zone to expand the algorithm's reach [53]-[56]. The decision mechanism guiding these behaviors is probabilistic if the parameter p exceeds a randomly generated threshold (rand), the gorilla ventures into unexplored terrain. If rand ≥ 0.5, it synchronizes its movement with peers, while rand < 0.5 triggers a focused shift toward a recognized location. These behavioral patterns serve as the foundation for the exploration model, and are formally expressed through the equation that follows.

$$GX^{(t+1)} = \begin{cases} (ub - lb)r_1 + lb & rand < p \\ (r_2 - C)X_r + LH & rand \geq 0.5 \\ X^{(i)} - L\left(LX^{(t)} - GX_r^{(t)}\right) + r_3\left(X^{(t)} - GX_r^{(t)}\right) & rand < 0.5 \end{cases} \quad (21)$$

In the subsequent iteration, $GX^{(t+1)}$ defines the updated position vector of a gorilla candidate, while $X^{(t)}$ denotes its current coordinates within the solution space. The indices r_1, r_2, r_3, and rand are random scalars drawn uniformly from the interval [0, 1]. The parameter p, ranging from 0 to 1, governs the likelihood of selecting one behavior over another. The symbols ub and lb establish the allowable bounds upper and lower for each decision variable in the search domain. X_r and GX_r signify gorilla individuals selected at random from the existing population. Key dynamics represented by C, H, and L are computed via equations that incorporate the current iteration count (it) and the total iterations allowed (it_{max}) during the optimization cycle [53].

$$C = F\left(1 - \frac{it}{it_{max}}\right) \; where \; \begin{cases} F = \cos(2r_4) + 1 \\ L = Cl \\ H = ZX^{(t)} \\ Z = [-C, C] \end{cases} \quad (22)$$

The variable r_4 introduces further randomness within [0, 1], while the cos function models oscillatory influence. Additionally, Z and l are randomized parameters drawn from the ranges $[-C, C]$ and $[-1, 1]$, respectively, injecting nonlinear variability into the process.As the exploration phase nears completion, the algorithm evaluates the fitness of each solution. Should the cost of the newly proposed location $GX^{(t)}$) prove superior (i.e., lower) to that of $X^{(t)}$, the update is accepted $GX^{(t)}$) replaces $X^{(t)}$, elevating it to the current best solution, metaphorically crowned as the Silverback. The strength of the algorithm lies in its twofold strategy: it casts a wide net to explore diverse possibilities, while simultaneously sharpening its focus through layered structures and competitive interactions. Inspired by the instinctive tactics gorillas use to navigate and solve problems in their environment, GTO encodes these behaviors into digital logic. The result is a sophisticated interplay between innovation and optimization, making it a powerful solution for tackling intricate optimization problems [54].

3.2 Exploitation phase

During the exploitation phase of the GTO, two distinct behavioral tactics come into play: shadowing the silverback and vying for the attention of adult females [53]. The algorithm dynamically selects one of these strategies based on a comparative evaluation between the parameter C from Eq. (23) and a predefined threshold value W.
When the value of C meets or exceeds the threshold W, the algorithm simulates the influence of the silverback the group's central authority figure. In the natural world, this dominant gorilla assumes the role of guide and protector, directing the troop toward optimal food sources. This behavior forms the basis of one exploitation mechanism, mathematically encapsulated in Eq. (23).

$$GX^{(t+1)} = LM\left(X^{(t)} - X_{silverbarck}^{t} + X^{(t)}\right) \quad (23)$$

$X^{(t)}$ and $X_{silverbarck}$ are the position-vector of the gorillas and the best solution, whereas symbols L and M can be calculated using (22) and (24).

$$M = \left(\left|\frac{1}{N}\sum_{i=1}^{N} GX^{(t)}\right|^{g}\right)^{\frac{1}{g}} \text{ where } \; g=2^{L} \quad (24)$$

Figure 1 illustrate how the positions of the agents representing individual gorillas are adjusted during the exploration phase, laying the groundwork for more refined movements during exploitation. In this context, $GX^{(t)}$ defines the location vector of each gorilla candidate at iteration *t*, with N denoting the total population. A secondary tactic comes into play when the condition C < W is met.

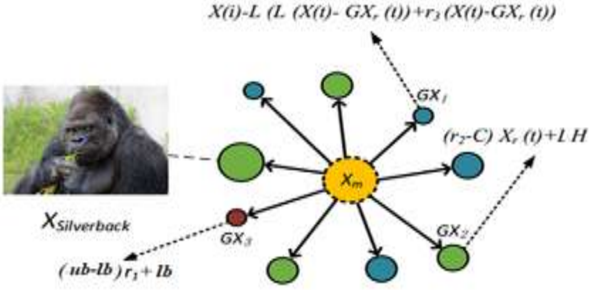

Figure 1. *Directions in the stage of exploration stage of GTO.*

As gorillas mature, younger males reach an age where they begin to challenge one another often aggressively to establish dominance and claim access to adult females [53], [55]. This natural competition, is captured analytically as

$$GX_i^{(t)} = X_{silverbarck} - (X_{silverbarck}Q - (X^{(t)}Q)A \quad (25)$$

$$where \begin{cases} Q = 2r_5 - 1 \\ A = \beta E \\ E = \begin{cases} N_1 & rand \geq 0.5 \\ N_2 & rand < 0.5 \end{cases} \end{cases}$$

$X_{silverbarck}$ in (25), represents the positional vector corresponding to the most optimal gorilla (silverback), while $X^{(t)}$ denotes the current location vector of a gorilla at iteration t. Q signifies the exerted impact force and is derived via Equation (25), with r_5 being a randomly generated scalar within the interval [0, 1]. The vector A quantifies the intensity of aggression in confrontational interactions. The parameter β is a predefined constant set before the optimization process begins. Additionally, the factor E is incorporated to model how violence influences the scaling of solution components. As the exploitation phase nears its conclusion, the values of fitness of all candidate solutions are reassessed. If $X^{(t)}$ is found to outperform that of $X^{(t)}$, then $GX^{(t)}$ replaces $X(t)$ and assumes the role of the best-known solution, effectively becoming the new silverback.

3.3 GTO-based EMO procedure

The application of GTO for OEM begins with the following stages:

Step 1: Specify the MG parameters, including DG units, storage device, and load profiles;
Step 2: Establish the optimization objective along with the corresponding operating constraints.
Step 3: Initialize the GTO settings like population size, decision variables, and maximum iterations.
Step 4: Randomly generate the initial search agents
Step 5: Calculate the exchanged power and check system constraints.
Step 6: Determine the fitness of each candidate;
Step 7: Update L and C using Eq. (22);
Step 8: Update location/position of gorilla using Eqs. (21), (23) and (25);
Step 9: Select the best candidate as the Silverback;
Step 10: Repeat the optimization process until the stopping criterion is satisfied;
Step 11: Output the optimal solution and stop.

3. Simulation, Results and Discussions

A simplified MG illustrating in Figure 2 was used to demonstrate the performance of the proposed model. The MG composed of various components like wind turbine (WT) connected at node 4, microturbines (MT) connected at node 7. Another includes a photovoltaic system (PV) connected at node 11, a fuel cell (FC) connected at node 23, and a diesel generator (DEG) connected at node 19.

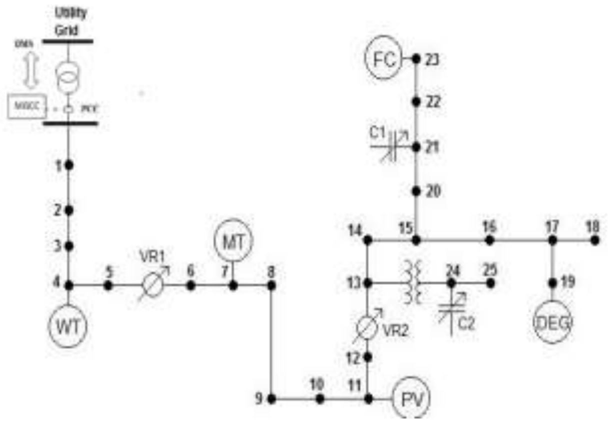

Figure 2. *One-line diagram of test system.*

To manage reactive power, capacitors compensation labeled C_1 and C_2 are connected at nodes 21 and 24, respectively, with a two voltage regulators labeled VR_1 connected between nodes 5 and 6, and VR_2 connected between nodes 12 and 13, respectively and a tap-changer transformer connected between nodes 13 and 24, respectively. The System highlights how different renewable and conventional energy sources are integrated and controlled within the MG, showing key control and power flow points for managing energy distribution and stability.

The GTO was applied to determine the optimal solution of the OEM problem in the microgrid, and its performance was validated through 10 independent simulation runs.

Within the MG, all available DG units supply power, while surplus or deficit energy is exchanged freely with the utility grid through the PCC. To evaluate the influence of electricity pricing, three market conditions were analyzed:

Case 1: Low market price;
Case 2: Average market price;
Case 3: Real-time market prices.

The proposed method was developed in MATLAB R2021a and executed on a Windows-10, 64-bit computer equipped with an Intel(R) Core(TM) i5-6500 processor and 8.0 GB RAM.

Forecast profiles of wind speed, temperature, and electricity prices over 24 hours are presented in Figure 3, while load demand was assumed to follow a daily variation pattern. Figures 4–7 illustrate the convergence behavior, total cost, DG outputs, utility power exchange, and operating daily cost results for the studied cases. Figures 8–10 display, respectively, charging/discharging battery for three cases, the state of charging battery (SoC) and daily cost for three cases of simulation.

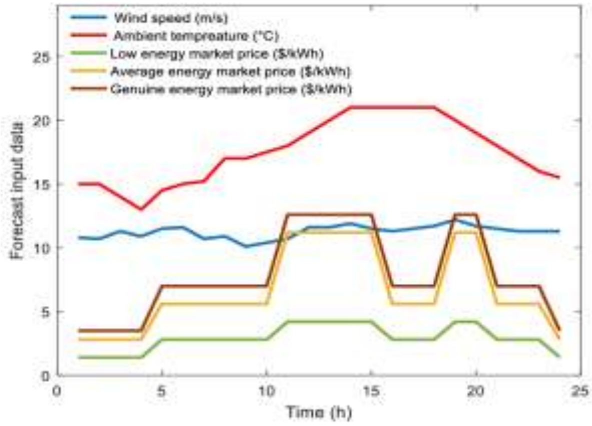

Figure 3. *Forecast input data's.*

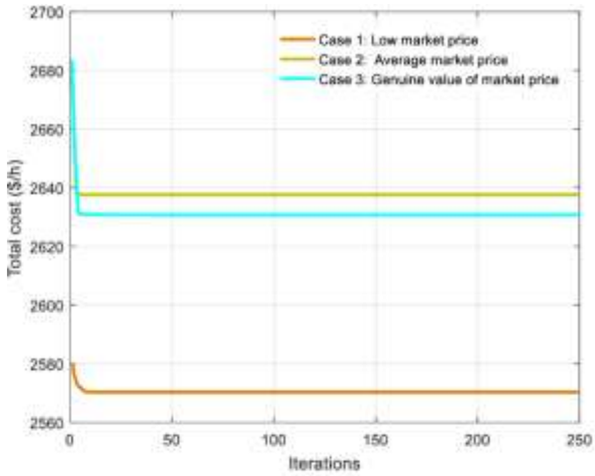

Figure 4. *Total cost for three cases.*

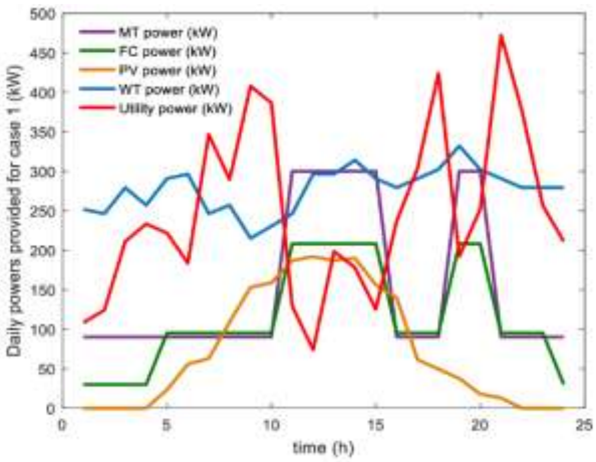

Figure 5. *Provided power of case 1.*

In Case 1, the low electricity price allows the utility grid to supply most of the MG demand, particularly during low and medium load periods, resulting in a minimum operating cost of 2570.29 ($/h).

For Case 2, with moderate market prices, the MT and fuel cell provide most of the required power. During average load conditions, surplus energy is transferred from the MG to the utility, leading to an operating cost of 2637.67 ($/h).

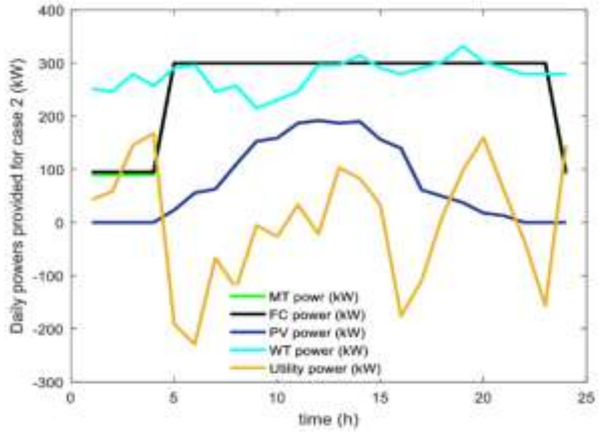

Figure 6. *Provided power of case 2.*

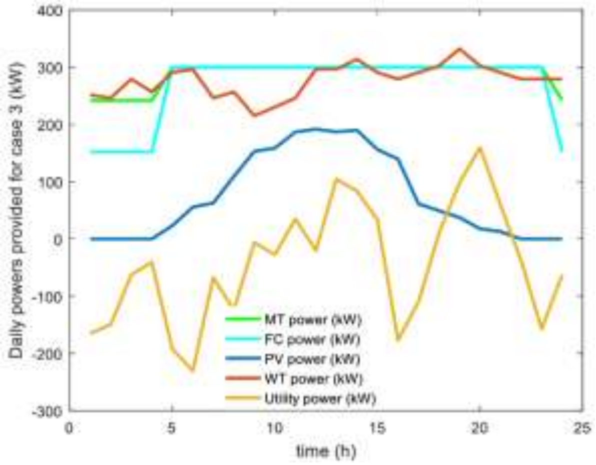

Figure 7. *Provided power of case 3.*

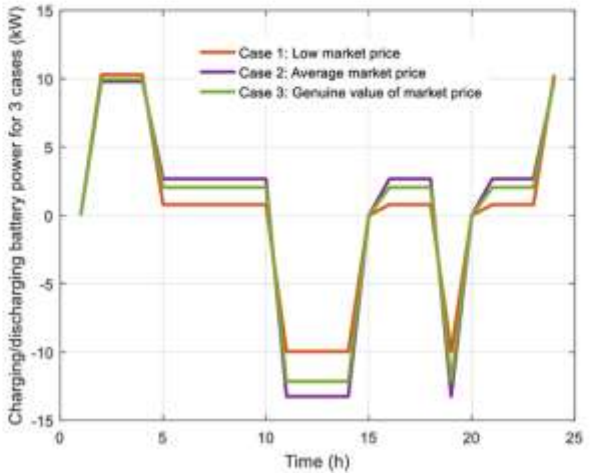

Figure 8. *Charging/discharging battery power for three cases.*

In Case 3, under real market prices, the MT and FC operate near full capacity during average and peak demand intervals, while excess power is exported to the grid for most of the day. The obtained optimal cost in this scenario is 2630.79 ($/h).

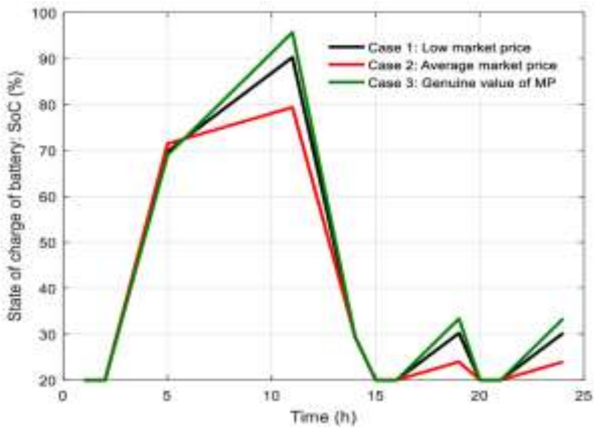

Figure 9. *State of charging battery: SoC.*

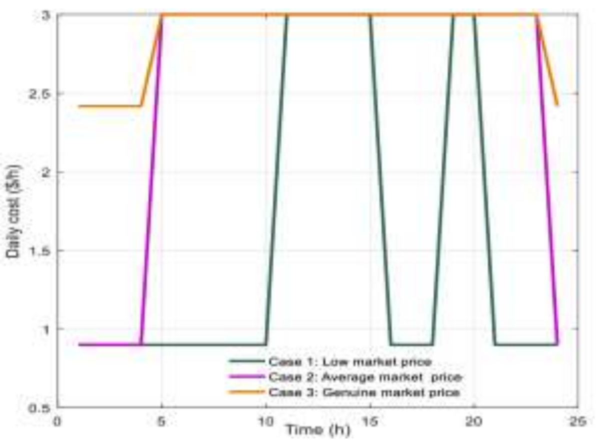

Figure 10. *Daily cost for three cases in ($/h).*

The simulation outcomes confirm the strong capability of the GTO in handling EMO for MGs. Compared with existing studies, the proposed method achieves superior solution quality with high robustness and efficient computational performance.

4. Conclusions

This study introduces a GTO based solution for MGs EMO. The method was tested on a MG integrating several DG and ESS under different operating conditions. Simulation findings demonstrate reliable and efficient EMO performance, with results comparable to or better than existing techniques reported in previous research.

Author Statements:

- **Ethical approval:** The conducted research is not related to either human or animal use.
- **Conflict of interest:** The authors declare that they have no known competing financial interests or personal relationships that could have appeared to influence the work reported in this paper
- **Acknowledgement:** The authors declare that they have nobody or no-company to acknowledge.
- **Author contributions:** The authors declare that they have equal right on this paper.
- **Funding information:** The authors declare that there is no funding to be acknowledged.
- **Data availability statement:** The data that support the findings of this study are available on request from the corresponding author. The data are not publicly available due to privacy or ethical restrictions.

References

[1] H. Wu, H. Li, X. Gu, "Optimal energy management for microgrids considering uncertainties in renewable energy generation and load demand," Processes, vol. 8, no. 9, p. 1086, 2020, doi:10.3390/pr8091086.
[2] H. Jiayi, J. Chuanwen, and X. Rong, "A review on distributed energy resources and MicroGrid," Renew. Sustain. Energy Rev., vol. 12, no. 9, pp. 2472–2483, 2008, doi: 10.1016/j.rser.2007.06.004.
[3] F. A. Mohamed, H. N. Koivo, "Online management genetic algorithms of microgrid for residential application," Energy Convers. Manag, vol. 64, pp. 562–568, 2012, doi:10.1016/j.enconman.2012.06.010.
[4] J. Radosavljević, M. Jevtić, and D. Klimenta, "Energy and operation management of a microgrid using particle swarm optimization," Eng. Optim., vol. 48, no. 5, pp. 811–830, 2016, doi:10.1080/0305215X.2015.1057135.
[5] C. Chen, S. Duan, T. Cai, B. Liu, G. Hu, "Smart energy management system for optimal microgrid economic operation," IET renewable power generation, vol. 5, no. 3, pp. 258–267, 2011, doi:10.1049/iet-rpg.2010.0052.
[6] A. Arabali, M. Ghofrani, M. Etezadi-Amoli, M. S. Fadali, and Y. Baghzouz, "Genetic-algorithm-based optimization approach for energy management," IEEE Trans. Power Deliv., vol. 28, no. 1, pp. 162–170, 2013, doi:10.1109/TPWRD.2012.2219598.
[7] K. F. Fong, V. I. Hanby, and T. T. Chow, "HVAC system optimization for energy management by evolutionary programming," Energy Build., vol. 38, no. 3, pp. 220–231, 2006, doi:10.1016/j.enbuild.2005.05.008.
[8] S. Mandal and K. K. Mandal, "Optimal energy management of microgrids under environmental constraints using chaos enhanced differential evolution," Renew. Energy Focus, vol. 34, pp. 129–141, 2020, doi:10.1016/j.ref.2020.05.002.
[9] Y. Li, S. Q. Mohammed, G. Saman, N. Aljojo, A. Rezvani, and S. Dadfar, "Energy Management of Microgrid considering Renewable Energy Sources and Electric Vehicles using Backtracking Search Optimization Algorithm," Journal of Energy Resources Technology, Transactions of the ASME, vol. 142, no. 5, pp. 1–18, 2020, doi:10.1115/1.4046098.

[10] Debata S, Samanta CK, Panigrahi SP ”Efficient energy management strategies for hybrid electric vehicles using shuffled frog-leaping algorithm,” International Journal of Sustainable Engineering, vol. 8, no. 2, pp. 138-144, 2013, doi:10.1080/19397038.2014.919363.

[11] R. Krishna, S. Hemamalini, ”Optimal Energy Management of Virtual Power Plants with Storage Devices Using Teaching-and-Learning-Based Optimization Algorithm,” International Transactions on Electrical Energy Systems, pp. 1-17, 2022, doi:10.1155/2022/1727524.

[12] M. Sedaghat, E. Rokrok, M. Bakhshipour, ”A Novel Method Based on Biogeography-Based Optimization for DG Planning in Distribution System,” Indonesian Journal of Electrical Engineering and Computer Science, vol. 15, no. 1, pp. 1-13, 2015, doi.org/10.11591/telkomnika.v15i1.8083.

[13] A. H. Kashan, ”League championship algorithm (LCA): an algorithm for global optimization inspired by sport championships,” Appl Soft Comput, vol. 16, pp. 171-200, 2014, doi.org/10.1016/j.asoc.2013.12.005.

[14] E. Lazar, A. Ignat, D. Petreus, R. Etz, ”Energy management for an islanded microgrid based on harmony search algorithm”, 41st International Spring Seminar on Electronics Technology (ISSE), pp. 16-20, 2018, doi:10.1109/ISSE.2018.8443673.

[15] M. M. Legha, F. Ostova, ”An imperialist competitive algorithm for sitting and sizing of distributed Generation in radial distribution network to improve reliability and losses reduction,” Iraqi Journal for Electrical and Electronic Engineering, vol. 9, no. 2, pp. 58-65, 2013, doi:10.37917/ijeee.9.2.3.

[16] I. Hussain, I. Ullah, R. Ramar, T. Tanzila, “Smart energy management system for university campus using sine-cosine optimization algorithm,“ International Virtual Conference on Power Engineering Computing and Control: Developments in Electric Vehicles and Energy Sector for Sustainable Future (PECCON), 05-06, 2022, doi:10.1109/PECCON55017.2022.9851066.

[17] A. Bahri, N. Mezhoud, B. Ayachi, F. Boukhenoufa, L. Bouras, “Multi-objective energy management and environmental index optimization of a microgrid using swarm intelligence algorithm, International Journal of Applied Power Engineering (IJAPE), vol. 13, no. 4, pp. 783-793, 2025, doi:10.11591/ijape.v14.i4.pp783-793.

[18] M. A. Kamarposhti, I. Colak, and K. Eguchi, “Optimal energy management of distributed generation in micro-grids using artificial bee colony algorithm,” Math. Biosci. Eng., vol. 18, no. 6, pp. 7402–7418, 2021, doi:10.3934/mbe.2021366.

[19] M. A. Kamarposhti H. Shokouhandeh, Y. Lee, S. K. Kang, I. Colak, E. M. Barhoumi, “Optimizing energy management in microgrids with ant colony optimization: enhancing reliability and cost efficiency for sustainable energy systems,“ International Journal of Low-Carbon Technologies, vol. 19, pp. 2848–2856, 2024, doi:10.1093/ijlct/ctae230.

[20] S. J. Ben Christopher, M. M. Carolin, “A bio-inspired approach for probabilistic energy management of micro-grid incorporating uncertainty in statistical cost estimation,“ Energy, vol. 203, no. p. 117810, 2020, doi:10.1016/j.energy.2020.117810.

[21] A. Nehmedo, K. Salah, F. M. Tamer, H. Maiya, M. A. Sobhy, “Developing an artificial hummingbird algorithm for probabilistic energy management of microgrids considering demand response,“ Frontiers in Energy Research, vol. 10, 2022,. doi:10.3389/fenrg.2022.905788.

[22] Y. Zhang, P. Liu, Y. Li, “Implementation of an enhanced crayfish optimization algorithm,“ Biomimetics, vol. 9, p. 341, 2024, doi:10.3390/biomimetics9060341.

[23] N. Mezhoud and M. Amarouayache, “Multi-objective optimal power flow based combined non-convex economic dispatch with valve-point effects and emission using gravitation search algorithm,” J. Appl. Res. Electr. Eng., vol. 2, no. 1, pp. 26–36, 2023, doi:10.22055/jaree.2022.40549.1055.

[24] H. R. E. H. Bouchekara, “Optimal power flow using black-hole-based optimization approach,“ Applied Soft Computing, vol. 24, no. 1, pp. 879–888, 2014, doi:10.1016/j.asoc.2014.08.056.

[25] N. Mezhoud, B. Ayachi, A. Bahri. “Wind driven optimization approach based multi-objective optimal power flow and emission index optimization,” International Research Journal of Multidisciplinary Technovation, vol. 4, no. 2, pp. 21-41, 2022, doi:10.54392/irjmt2223

[26] R. Sanket, N. Thangadurai, “Optimal Power Flow for Distribution System using Gradient-Based Optimizer,“ International Journal of Electrical and Electronics Research, vol. 11, no. 3, pp. 711-719, 2023, doi:10.37391/ijeer.110311.

[27] M. Ankur, R. S. Yog, J. Supriya, “Flow direction algorithm-based optimal power flow analysis in the presence of stochastic renewable energy sources,“ Electric Power Systems Research, vol. 216, p. 109087, doi:10.1016/j.epsr.2022.109087.

[28] N. Mezhoud, “Multi-objective optimal power flow and emission index based firefly algorithm,” Period. Polytech. Electr. Eng. Comput. Sci., vol. 67, no. 2, pp. 172–180, 2023, doi:10.3311/PPee.20922.

[29] Y. Sun, X. Wang, L. Gao, H. Yang, K. Zhang, H. Zhang, “Multi-Objective Optimal scheduling for microgrids—improved goose algorithm,“ Energies, vol. 17, no. 24, p. 6376, 2024, doi:10.3390/en17246376.

[30] N. Mezhoud, A. Bahri, B. Ayachi, F.Boukhenoufa, L. Bouras, “Energy management optimization and optimal control of microgrid enriched with renewable and sustainable distributed generators using nature-inspired method”, ITEGAM-JETIA, vol. 11, no. 54, pp. 215–230, 2025, doi: 10.5935/jetia.v11i54.1767.

[31] A. M. Rafi, M. Ali, M. I. Hossain, F. A., Sulaiman, M. Shafiullah, “Whale Optimization Algorithm for Community Microgrid Energy Scheduling,“ Saudi Arabia Smart Grid (SASG), 12-14 december 2022, doi:10.1109/SASG57022.2022.10200591.

[32] B. Hernández-Ocaña, J. Hernández-Torruco, O. Chávez-Bosquez, M. B. Calva-Yáñez, and E. A.

Portilla-Flores, "Bacterial foraging-based algorithm for optimizing the power generation of an isolated microgrid," Appl. Sci., vol. 9, no. 6, 2019, doi:10.3390/app9061261.

[33] Y. M. Alsmadi et al., "Optimal configuration and energy management scheme of an isolated micro-grid using Cuckoo search optimization algorithm," J. Franklin Inst., vol. 356, no. 8, pp. 4191–4214, 2019, doi:10.1016/j.jfranklin.2018.12.014.

[34] B. N. Kommula, H. Song, L. Chen, Ch. Xu, "Efficient energy management of hybrid renewable energy sources-based smart-grid system using a hybrid IDEA-CFA technique," International Transactions on Electrical Energy Systems, vol. 31, no. 1, 2021, doi:10.1002/2050-7038.12833.

[35] B. Bentouati, A. Khelifi, A. M. Shaheen, R. A. El-Sehiemy, "An enhanced moth-swarm algorithm for efficient energy management based multi dimensions OPF problem," J. Ambient Intell. Humaniz. Comput., vol. 12, no. 10, pp. 9499–9519, 2021, doi:10.1007/s12652-020-02692-7.

[36] K. Mohit, K. Ashwani, K. Sunil, C. Piyush, S. Shitharth, "An African vulture optimization algorithm based energy efficient clustering scheme in wireless sensor networks," Scientific Reports, vol. 14, p.31412, doi:10.1038/s41598-024-83005-2.

[37] S, Mouassa, M. Saida, C. Djabali, F. Jurado, "Optimal power flow solution based on gorilla troops optimization technique considering uncertainty of renewable energy sources: A case study of Adrar's isolated power network," Wind Engineering, vol. 47, pp. 1–22, 2023, doi:10.1177/0309524X231163826.

[38] A. Kheiter, S. Souag, A. Chaouch, A. Boukortt, B. Bekkouche, M. Guezgouz, "Energy Management Strategy Based on Marine Predators Algorithm for Grid-Connected Microgrid," International Journal of Renewable Energy Development, vol. 11, no. pp. 751-765, 2022, doi:10.14710/.

[39] K. Roy, K. K. Mandal, A. C. Mandal, "Ant-Lion Optimizer algorithm and recurrent neural network for energy management of micro grid connected system," Energy, vol. 167: pp. 402-416, 2019, doi:10.1016/j.energy.2018.10.153.

[40] E. Lodhi, F. Y. Wang, G. Xiong, C. A. Mallah, M. Y. Javed, T. S. Tamir, D. W. Gao, "Dragonfly Optimization Algorithm for Extracting Maximum Power of Grid-Interfaced PV Systems," Sustainability, vol. 13, no. 19, 2021, doi:10.3390/su131910778.

[41] J. Radosavljević, "Metaheuristic optimization in power engineering," The Institution of Engineering and Technology, Michael Faraday House, Six Hills Way, Stevenage, Herts, SG1 2AY, United Kingdom, 2018, doi:10.1049/PBPO131E.

[42] Y. Zhang, N. Gatsis, and G. B. Giannakis, "Robust energy management for microgrids with high-penetration renewables," IEEE Trans. Sustain. energy, vol. 4, no. 4, pp. 944–953, 2013, doi:10.1109/TSTE.2013.2255135.

[43] H. Wu, X. Liu, and M. Ding, "Dynamic economic dispatch of a microgrid: Mathematical models and solution algorithm," Int. J. Electr. Power Energy Syst., vol. 63, pp. 336–346, 2014, doi:10.1016/j.ijepes.2014.06.002.

[44] P. Samarjit, R. N. Manas, V. Meera, "Smart deployment of energy storage and renewable energy sources for improving distribution system efficacy," AIMS Electronics and Electrical Engineering, vol. 6, no. 4, pp. 397–417, 2022, doi.10.3934/electreng.2022024.

[45] A. A. Moghaddam, A. Seifi, T. Niknam, and M. R. A. Pahlavani, "Multi-objective operation management of a renewable MG (micro-grid) with back-up micro-turbine/fuel cell/battery hybrid power source," Energy, vol. 36, no. 11, pp. 6490–6507, 2011, doi:10.1016/j.energy.2011.09.017.

[46] A. M. Azmy and I. Erlich, "Online optimal management of PEMFuel cells using neural networks," IEEE Trans. Power Deliv., vol. 20, no. 2, pp. 1051–1058, 2005, doi:10.1109/PES.2005.1489132.

[47] S. Campanari, E. Macchi, "Technical and tariff scenarios effect on microturbine trigenerative applications," Journal of Engineering for Gas Turbines and Power, vol. 126, no. 3, pp. 581–589, 2004, doi:10.1115/1.1762904.

[48] F. Barbir, T. Gómez, "Efficiency and economics of proton exchange membrane (PEM) fuel cells. International Journal of Hydrogen," Energy, vol. 22, no, 10, pp. 1027–1037, 1997, doi:10.1016/S0360-3199(96)00175-9.

[49] D. Villanueva, J. L. Pazos, A. Feijo, "Probabilistic load flow including wind power generation," IEEE Transactions on Power Systems, vol. 26, no. 3, pp. 1659–1667. doi:10.1109/TPWRS.2010.2096436.

[50] Y. M. Atwa, E. F. El-Saadany, M. M. A. Salama, R. Seethapathy, M. Assam, S. Conti, "Adequacy evaluation of distribution system including wind/solar DG during different modes of operation, IEEE Transactions on Power Systems, 26, no. 4, vol. pp. 1945–1952. doi:10.1109/TPWRS.2011.2112783.

[51] G. N. Tiwari, S. Dubey, "Fundamentals of photovoltaic modules and their applications. London: RSC Energy Series Cambridge, "ebook collection, ECCC Environmental eBooks, pp. 1968-2022, doi:10.1039/9781849730952.

[52] B. Abdollahzadeh, G. F. Soleimanian, S. Mirjalili, "Artificial gorilla troops optimizer: A new nature inspired metaheuristic algorithm for global optimization problems," International Journal of Intelligent Systems, vol. 36, pp. 5887–5958, 2021, doi:10.1002/int.22535.

[53] E. H. Houssein, M. R. Saad, A. A. Ali, H. Shaban, "An efficient multi-objective gorilla troops optimizer for minimizing energy consumption of large-scale wireless sensor networks," Expert Systems with Applications, vol. 212, p. 118827, 2014, doi:10.1016/j.eswa.2022.118827.

[54] A. M. Shaheen, A. Ginidi, R. A.E l-Sehiemy, H. T. Dorrah, "Developed Gorilla Troops Technique for Optimal Power Flow Problem in Electrical Power Systems," Mathematics, vol. 10, p. 1636 2022, doi:10.3390/math10101636.

[55] H. A. Mohammed, Z. A. Sulaiman, S. A. Ali,, R. G. Ahmed M. S. Abdullah, "Enhanced power grid

performance through Gorilla Troops Algorithm-guided thyristor controlled series capacitors allocation," Heliyon, vol. 10, no. 14, pp. 1-30, 2024, doi:10.1016/j.heliyon.2024.e34326.

[56] A. Ginidi,S. M. Ghoneim, A. Elsayed, R. El-Sehiemy, A. Shaheen, A. El-Fergany, "Gorilla Troops Optimizer for Electrically Based Single and Double-Diode Models of Solar Photovoltaic Systems," Sustainability, vol. 13, no. 16, pp. 2-28, 2024, doi:10.3390/su13169459.